AMERICAN SOCIETY FOR MICROBIOLOGY | Journal of Virology®

Isolation and Characterization of vΔI3 Confirm that Vaccinia Virus SSB Plays an Essential Role in Viral Replication

Matthew D. Greseth,[a] Maciej W. Czarnecki,[a] Matthew S. Bluma,[b] Paula Traktman[a,c]

[a]Departments of Biochemistry and Molecular Biology, Medical University of South Carolina, Charleston, South Carolina, USA

[b]Department of Microbiology and Immunology, Medical College of Wisconsin, Milwaukee, Wisconsin, USA

[c]Department of Microbiology and Immunology, Medical University of South Carolina, Charleston, South Carolina, USA

ABSTRACT Vaccinia virus is unusual among DNA viruses in replicating exclusively in the cytoplasm of infected cells. The single-stranded DNA (ssDNA) binding protein (SSB) I3 is among the replication machinery encoded by the 195-kb genome, although direct genetic analysis of I3 has been lacking. Herein, we describe a complementing cell line (CV1-I3) that fully supports the replication of a null virus (vΔI3) lacking the I3 open reading frame (ORF). In noncomplementing CV1-CAT cells, vΔI3 shows a severe defect in the production of infectious virus (≥200-fold reduction). Early protein synthesis and core disassembly occur normally. However, DNA replication is profoundly impaired (≤0.2% of wild-type [WT] levels), and late proteins do not accumulate. When several other noncomplementing cell lines are infected with vΔI3, the yield of infectious virus is also dramatically reduced (168- to 1,776-fold reduction). Surprisingly, the residual levels of DNA accumulation vary from 1 to 12% in the different cell lines (CV1-CAT < A549 < BSC40 < HeLa); however, any nascent DNA that can be detected is subgenomic in size. Although this subgenomic DNA supports late protein expression, it does not support the production of infectious virions. Electron microscopy (EM) analysis of vΔI3-infected BSC40 cells reveals that immature virions are abundant but no mature virions are observed. Aberrant virions characteristic of a block to genome encapsidation are seen instead. Finally, we demonstrate that a CV1 cell line encoding a previously described I3 variant with impaired ssDNA binding activity is unable to complement vΔI3. This report provides definitive evidence that the vaccinia virus I3 protein is the replicative SSB and is essential for productive viral replication.

IMPORTANCE Poxviruses are of historical and contemporary importance as infectious agents, vaccines, and oncolytic therapeutics. The cytoplasmic replication of poxviruses is unique among DNA viruses of mammalian cells and necessitates that the double-stranded DNA (dsDNA) genome encode the viral replication machinery. This study focuses on the I3 protein. As a ssDNA binding protein (SSB), I3 has been presumed to play essential roles in genome replication, recombination, and repair, although genetic analysis has been lacking. Herein, we report the characterization of an I3 deletion virus. In the absence of I3 expression, DNA replication is severely compromised and viral yield profoundly decreased. The production of infectious virus can be restored in a cell line expressing WT I3 but not in a cell line expressing an I3 mutant that is defective in ssDNA binding activity. These data show conclusively that I3 is an essential viral protein and functions as the viral replicative SSB.

KEYWORDS DNA replication, I3, SSB, complementing cell line, deletion virus, molecular genetics, poxvirus, vaccinia virus

Received 2 October 2017 **Accepted** 20 October 2017

Accepted manuscript posted online 1 November 2017

Citation Greseth MD, Czarnecki MW, Bluma MS, Traktman P. 2018. Isolation and characterization of vΔI3 confirm that vaccinia virus SSB plays an essential role in viral replication. J Virol 92:e01719-17. https://doi.org/10.1128/JVI.01719-17.

Editor Rozanne M. Sandri-Goldin, University of California, Irvine

Copyright © 2018 American Society for Microbiology. All Rights Reserved.

Address correspondence to Paula Traktman, traktman@musc.edu.

M.D.G. and M.W.C. contributed equally to this article.

Vaccinia virus, the prototypic poxvirus, is a complex double-stranded DNA (dsDNA) virus with a genome of 195 kb (1). One of the most distinguishing features of vaccinia virus is that it replicates solely within the cytoplasm of infected cells. This physical autonomy from the nucleus is accompanied by significant genetic autonomy from the cell. Vaccinia virus encodes a repertoire of proteins that are required for the replication of the viral genome (2, 3). These include the catalytic DNA polymerase (E9) and its heterodimeric processivity factor, which is comprised of the A20 protein and the D4 protein, an enzymatically active uracil DNA glycosylase (4, 5). In addition, the virus encodes the D5 protein, a hexameric AAA+ ATPase that has all of the sequence hallmarks of an SFIII helicase and has an N′-terminal primase domain (6, 7). The H5 protein is an abundant phosphoprotein that interacts with numerous binding partners, including other replication proteins, DNA and RNA, and membranes (8, 9); we have recently reported that the deletion virus vΔH5 shows a profound block to DNA replication in noncomplementing cells (10). The G5 protein is a member of the FEN-1-like family of structure-specific nucleases, and in its absence, the integrity of replication products is compromised. The vast majority of the DNA that accumulates during vΔG5 infections is subgenomic in size (45 to 150 kb) (11; M. W. Czarnecki and P. Traktman, unpublished data). The viral A50 protein is a DNA ligase, and it too is essential for viral DNA replication in those circumstances in which the cellular DNA ligase I is not available; an enzymatically active DNA ligase is needed for productive infection (12; Czarnecki and Traktman, unpublished). Finally, the I3 protein is a single-stranded DNA (ssDNA) binding protein (SSB) (13–16), and it is the focus of the work described herein.

I3, unlike most SSBs, does not have a recognizable OB fold, and the sequence bears little or no similarity to those of any prokaryotic or eukaryotic SSBs. A conserved stretch of aromatic and basic residues suggests that I3 might retain some of the ssDNA-interacting interface of other SSBs (15), but this is far from clear. Bioinformatic analysis suggests that I3 most likely evolved from the SmpB family of prokaryotic proteins, which interact with transfer-messenger RNA (tmRNA), a molecule that has both tRNA and mRNA functions (17). The central region of I3 models well on the SmpB structure and overlaps with several motifs that are highly conserved among poxvirus orthologs and have been shown to be important for DNA binding and I3-I3 interactions *in vitro* (15). Like many other SSBs, the vaccinia virus I3 protein has an acidic C′-terminal tail. However, whereas this tail is thought to mediate protein-protein interactions in other cases, it has recently been shown that for I3, the C′ terminus modulates the interaction of the protein with DNA (16). Truncation of the tail increases the affinity of I3 for DNA and appears to alter the structure of DNA-I3 complexes, leading to the hypothesis that the C′ terminus may normally facilitate the sliding of I3 on DNA during replication.

The I3 protein is highly conserved among different orthopoxviruses and is expressed at early and intermediate times postinfection; we have not detected I3 as a component of purified virions. The 34-kDa I3 protein is phosphorylated on serine residues (13), although the sites of phosphorylation have not been mapped. I3 preparations purified from infected cells and recombinant I3 purified from *Escherichia coli* bind ssDNA tightly and with great specificity (13). SSBs play a central role in all known DNA replication systems, and I3 has been presumed to serve the role of the replicative SSB for poxviruses. I3 is highly concentrated within replication factories (13, 15, 18) and expressed at the correct time during infection to support genome replication. Temperature-sensitive (*ts*) mutants with lesions in I3 were not recovered in the Condit-Dales collections (19), and more recent studies from our lab, using clustered charge-to-alanine mutagenesis of I3, also failed to yield *ts* mutants (15). Small interfering RNA (siRNA) depletion of I3 has been shown to diminish DNA replication, DNA recombination, and viral yield (15, 20), but the magnitude of the impact was less than might have been expected, with DNA replication being reduced 4- to 7-fold. Given that a fraction of cells fail to take up the transfected siRNA and that some residual I3 remains even in affected cells, it is difficult to know whether the modest impact is due to the limitations of the technical approach or to the fact that I3 might not be essential for replication. Finally, I3 has been shown to associate with the

viral genome immediately upon its release from the disassembling core, even under circumstances in which DNA replication itself cannot initiate (21, 22). Whether the newly released parental genome has significant single-stranded character or whether this association is indirect and due to protein-protein interactions is not known.

As a more definitive approach to studying the role of I3 in the vaccinia virus life cycle, we describe herein our construction of an I3-expressing cell line and the subsequent construction of a deletion virus lacking I3 (vΔI3). Our analysis of vΔI3 reveals that I3 is essential for productive viral infection. In its absence, full-length progeny genomes do not accumulate, and the yield of infectious virus is greatly reduced. These conclusions hold true for the four cell lines that were tested, although intriguing phenotypic differences were observed in the different cell lines.

RESULTS

Generation of an I3-expressing cell line. As described above, although we have utilized a variety of techniques to assess the contribution of I3 to the viral life cycle (15), our genetic studies have been hampered by the lack of a temperature-sensitive mutant and the caveats that attend siRNA-mediated depletion of the abundant I3 protein. Therefore, with the goal of generating an I3 deletion mutant (vΔI3), we first generated a cell line that expresses I3 in an inducible manner (CV1-I3). We used the Flp-In system, which allowed us to insert a single, inducible I3 transgene in a common genomic locus. The I3 transgene was codon optimized for expression from the nuclear genome. We were successful in generating a cell line that expressed I3 in the presence, but not the absence, of doxycycline (DOX), as shown in Fig. 1A. The levels expressed in the presence of doxycycline are 2.5-fold (±0.15-fold) greater than what is seen during a wild-type (WT) infection; this level of expression is similar to what we observed for the H5, F10, and G5 viral proteins using this system (10, 23; Czarnecki and Traktman, unpublished). The I3 protein was also visualized by immunofluorescence; no protein was detected in uninduced CV1-I3 cells, but I3 was readily visualized throughout the cytoplasm of induced cells (Fig. 1B). In the results presented below, infections performed in CV1-I3 cells are compared with those performed in a control cell line (CV1-CAT) that expresses an unrelated protein (chloramphenicol acetyltransferase).

Generation of the vΔI3 deletion virus: I3 is essential for viral replication. With the CV1-I3 cell line in hand, we utilized homologous recombination to isolate vΔI3, a virus in which the I3 allele (except for the embedded I2 promoter) has been replaced with the fluorescent reporter red fluorescent protein (RFP). A schematic of the genomic locus of the WT genome and the targeted allele is shown in Fig. 1C. Recombinant plaques were isolated by iterative rounds of plaque purification until all progeny plaques were RFP positive. The absence of any residual WT virus was confirmed by PCR analysis (data not shown).

Our initial characterization of vΔI3 involved the assessment of plaque formation and one-step growth yields. As shown in Fig. 1D, WT virus produced plaques of comparable size on the control CV1-CAT cells and the CV1-I3 cells in the presence of doxycycline. In contrast, vΔI3 produced macroscopic plaques only in the induced CV1-I3 cells (bottom right well); none were visible in the induced CV1-CAT cells (bottom left well). The yield of infectious virus from a single replicative cycle (multiplicity of infection [MOI] of 5, 18 h postinfection [hpi]) was also assessed (Fig. 1E). Whereas WT virus produced comparable yields in both the CV1-CAT and CV1-I3 cell lines in the absence or presence of doxycycline, vΔI3 exhibited a very different phenotype. The viral yield from infections of CV1-CAT cells (with or without DOX) or uninduced CV1-I3 cells was ~250- to 550-fold lower than what was produced in induced CV1-I3 cells. These data indicate that the deletion virus is highly impaired in its replication and that this defect is due solely to the absence of I3 expression from the viral genome.

Phenotypic characterization of the replicative defect of vΔI3 in noncomplementing cells. (i) Early gene expression and the accumulation of replication proteins. Our next step was to characterize the early stages of viral infection, beginning with the expression and accumulation of the early proteins that are known components

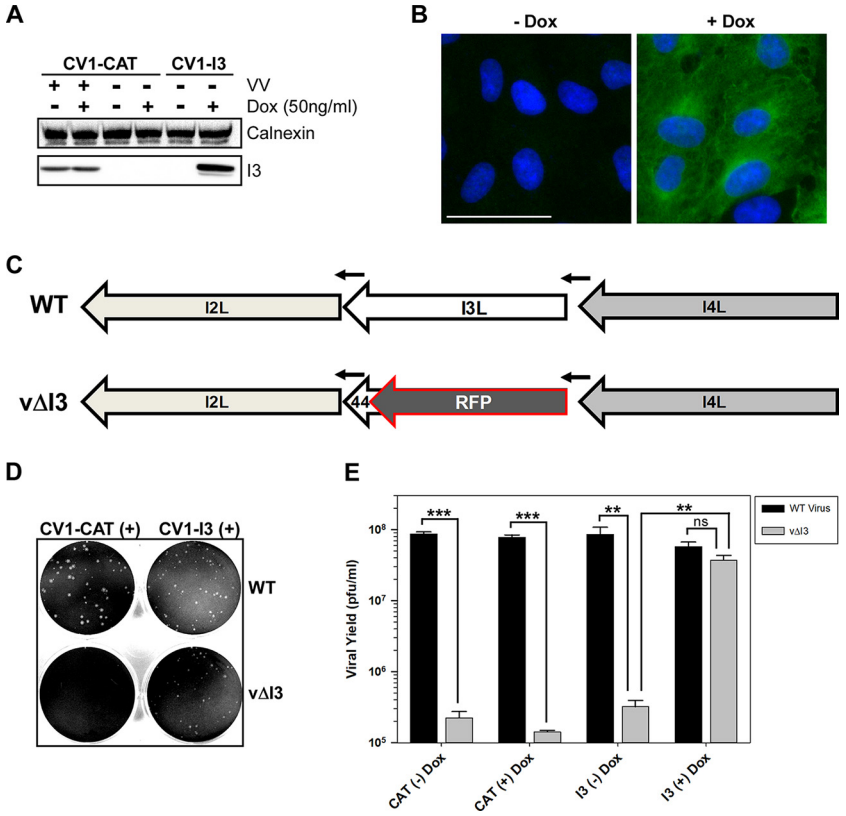

FIG 1 Deletion of I3 severely impairs viral yield. (A) Generation of an I3-expressing cell line (CV1-I3) allows for exogenous accumulation of I3 at levels approximating those seen during a WT infection. CV1-CAT and CV1-I3 cells were left untreated (−) or treated with 50 ng/ml doxycycline (+) for 24 h. Additionally, CV1-CAT cells were infected with WT virus (MOI, 5) for 24 h. Fifty micrograms of total protein was resolved, and I3 accumulation was quantified ($n = 3$; a representative immunoblot is shown). (B) CV1-I3 cells accumulate exogenous I3 throughout the cytoplasm. CV1-I3 cells were left untreated (left panel) or treated with 50 ng/ml doxycycline (right panel) for 24 h and stained with DAPI (blue) and I3 (green). Scale bar, 200 μm. (C) Schematic representation of the targeted region of the vΔI3 genome. Leftward arrows represent promoter regions. (D) No macroscopic plaques are seen in the absence of I3. CV1-CAT (left) and CV1-I3 (right) cells were treated with 50 ng/ml doxycycline for 24 h. Cells were then infected with 50 PFU of WT virus (top) or vΔI3 (bottom) for 48 h and stained with crystal violet. (E) Loss of I3 has a dramatic impact on viral yield. CV1-CAT and CV1-I3 cells were either left untreated [(−) Dox] or treated with 50 ng/ml doxycycline [(+) Dox] for 24 h. Cells were then infected with the WT virus (black bars) or vΔI3 (gray bars) (MOI, 5) for 18 h. Viral yield is plotted as the average from three experiments. Error bars represent standard error of the mean (**, $P < 0.02$; ***, $P < 0.001$).

of the replication machinery. These analyses were performed using CV1-CAT and CV1-I3 cells. As shown in Fig. 2A, the accumulation of the D5, A20, H5, and Pol (not shown) proteins were comparable in cells infected with WT virus and vΔI3, indicating that viral entry and early gene expression occur normally in the absence of I3 expression. Interestingly, however, in the absence of I3, the H5 band was sharp and distinct, which was qualitatively different from what was seen in the WT samples. Although H5 is phosphorylated throughout infection, only those modifications that occur after the onset of late protein expression cause electrophoretic mobility shifts (24). The absence of these modifications in the vΔI3 sample suggests that the biochemical progression of the life cycle might be incomplete in the absence of I3.

(ii) Core disassembly. Core disassembly is the next step of the viral life cycle, and we assessed this process in CV1-CAT cells using an immunofluorescence assay that relies upon visualization of the A5 protein in intact cores or after core wall dispersal (10, 22). The expression of early proteins is a prerequisite for core disassembly, and when cells are infected in the presence of cycloheximide and then stained with anti-A5 (a core wall marker) at 3 hpi, the cores can be seen as bright puncta throughout the cytoplasm

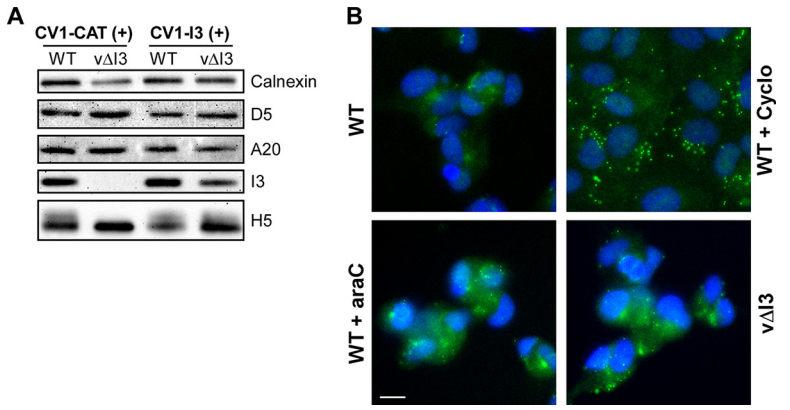

FIG 2 Early events of the viral life cycle occur normally in the absence of I3. (A) Essential early viral replication proteins accumulate to WT levels during vΔI3 infection. CV1-CAT and CV1-I3 cells were induced with 50 ng/ml doxycycline. Induced cells were infected with WT or vΔI3 virus (MOI, 5) for 18 h. Cell lysates were resolved electrophoretically and probed for calnexin (loading control) as well as the replication proteins D5, A20, I3, and H5. A representative immunoblot is shown. (B) Uncoating (core disassembly) is unperturbed during a vΔI3 infection. CV1-CAT cells were infected with WT virus (top left panel) or vΔI3 (bottom right panel) (MOI, 15) for 3 h. Additionally, cells were infected with WT virus (MOI, 15) in the presence of cycloheximide (Cyclo) (25 μg/ml) (top right panel) or araC (20 μM) (lower left panel). Cells were then fixed and stained with DAPI (blue) and the viral core protein A5 (green). Scale bar, 50 μm; representative images are shown.

(Fig. 2B, upper right panel). In contrast, in cells infected with WT virus in the absence of inhibitors, a diffuse cytoplasmic pattern of staining is seen, along with one larger perinuclear focus of A5 staining (upper left panel). This same staining pattern is seen in the presence of cytosine arabinoside (araC) (lower left panel), because core disassembly precedes and is independent of the onset of DNA replication. When vΔI3 infections were examined (lower right panel), the profile was similar to that seen during WT infections in the absence of inhibitors (or in the presence of araC) and dissimilar from that seen with cycloheximide. These data indicate that I3 expression is not required for core disassembly.

(iii) DNA replication. Given the extensive characterization of I3 as a single-stranded DNA binding protein and the demonstration of its accumulation within replication factories (13–16, 18, 20), we anticipated that it would play a key role in DNA replication. A temporal profile of DNA accumulation during WT and vΔI3 infections of CV1-CAT cells is illustrated in Fig. 3A, with both the image of the Southern dot blot filter and the graphical analysis shown. A typical curve of DNA replication is seen in the WT samples, with a linear increase in DNA accumulation seen between 4 and 10 hpi and a more modest increase seen thereafter. In vΔI3 infections, the absence of DNA accumulation is striking, with the levels being $<$0.2% of those seen for WT samples at each time point. We also utilized pulse-field gel electrophoresis (PFGE) to visualize the accumulation of viral DNA (Fig. 3B) throughout infection. A robust signal for the 195-KB viral genome (arrow) was observed in the samples harvested from WT infections from 6 to 24 hpi, but no signal was seen in the vΔI3 samples, by either ethidium bromide (EtBr) staining (not shown) or Southern blot hybridization. Taken together, the data shown in Fig. 3A and B indicate that the absence of I3 expression drastically impairs DNA replication.

(iv) Late gene expression. The transcription of intermediate and late genes, and hence the expression of the encoded proteins, is not seen when infections are performed in the presence of araC, a stringent inhibitor of DNA synthesis. We therefore anticipated that the temporal cascade of protein expression would be impaired during vΔI3 infection. As an initial assessment, we pulse-labeled CV1-CAT cells infected with WT virus or vΔI3 with [^{35}S]methionine at intervals from 0.75 to 6.75 hpi to visualize the profile of nascent proteins (Fig. 3C). The typical profile was seen in WT-infected cells: host proteins (*) begin to decline in synthesis soon after infection, and early (●), intermediate (△), and late (○) proteins appear in succession. In contrast, the decline in

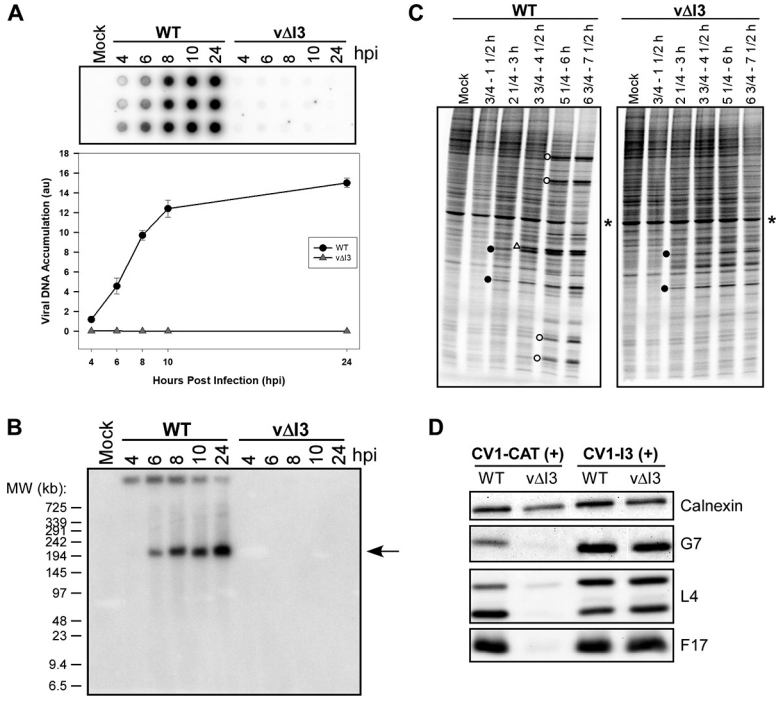

FIG 3 Later events of the viral life cycle (DNA replication and late protein accumulation) are significantly impaired in the absence of I3. (A and B) Viral DNA replication is absent upon loss of I3. CV1-CAT cells were infected with WT virus or vΔI3 (MOI, 5) and collected at the designated times (4 to 24 hpi). (A) Cell lysates were processed for Southern dot blot analysis. Samples were spotted in technical triplicate (upper panel); a representative blot is shown. DNA accumulation was quantified and graphed (lower panel). Data are plotted as the average from three biological experiments. (B) Additionally, samples were processed for PFGE followed by Southern blotting. A representative image is shown; the arrow represents accumulation of full-length genome. (C and D) Late protein synthesis is severely diminished. (C) CV1-CAT cells were infected with WT or vΔI3 virus (MOI, 5) and pulse-labeled with [^{35}S]methionine at the indicated times. Samples were resolved electrophoretically and proteins visualized by phosphorimaging. A representative image is shown (*, host protein; ●, early; △, intermediate; ○, late). (D) CV1-CAT and CV1-I3 cells were induced with 50 ng/ml doxycycline and infected with WT or vΔI3 (MOI, 5) for 18 h. Cell lysates were subjected to immunoblot analysis and probed for calnexin, G7, L4, and F17. A representative blot is shown.

host protein synthesis was delayed and minimal during vΔI3 infections, and only early proteins could be readily seen. We next compared the accumulation of representative late proteins (L4, G7, and F17) in WT versus vΔI3 infections by immunoblot analysis, and we observed that these proteins were either absent or present at trace levels during vΔI3 infections of CV1-CAT cells (Fig. 3D). (L4 is a major core protein that undergoes proteolytic cleavage during virion morphogenesis; both the 29-kDa precursor and 25-kDa mature product are detected by the antibody. F17 is a major virion component that has been referred to as F18 in earlier literature [25, 26].) Furthermore, accumulation of late proteins was restored during infections of preinduced CV1-I3 cells. In sum, in CV1-CAT cells, vΔI3 has a characteristic "DNA$^-$" phenotype, in which early events of infection proceed normally, but no DNA is synthesized and the accumulation of postreplicative proteins and infectious virions is absent.

Comparison of the vΔI3 phenotype in a variety of cell lines. Because vaccinia virus replicates exclusively in the cytoplasm of infected cells and encodes a large repertoire of replication enzymes, a role for nuclear functions in genome synthesis has largely been discounted. However, a possible role for the involvement of cellular proteins in genome replication, with host range implications, can be inferred from some published reports (27–29). We therefore infected several different cell lines with vΔI3 to assess any differences in phenotype.

(i) Infectious viral yield from a single infectious cycle. BSC40, HeLa, A549, and CV1-CAT cells were infected with WT virus and vΔI3, and the yield from a single cycle

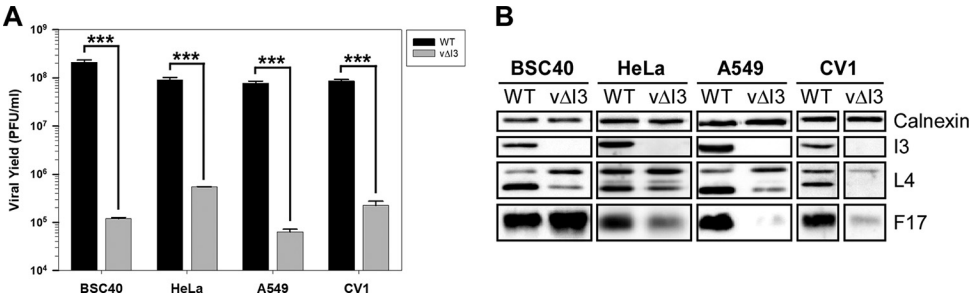

FIG 4 Loss of I3 has a severe impact in several different cell lines. (A) Loss of I3 decreases viral yield in several cell lines. BSC40, HeLa, A549, and CV1-CAT cells were infected with WT virus (black bars) or vΔI3 (gray bars) (MOI, 5) for 18 h. The viral yield is plotted as the average from three experiments. Error bars represent standard error of the mean (***, $P < 0.001$). (B) Loss of I3 has a varied impact on late protein accumulation in various cell lines. BSC40, HeLa, A549, and CV1-CAT cells were infected with WT virus or vΔI3 (MOI, 5) for 18 h. Cell lysates were processed for immunoblot analysis using calnexin, I3, L4, and F17 antisera. A representative blot is shown.

of infection was assessed. The replication of vΔI3 was severely impaired in all cell lines tested. Relative to the yield of WT virus produced in each cell line, the yield of vΔI3 was reduced by 1,176-, 168-, 1,233-, and 386-fold, respectively (Fig. 4A) (average of 3 replicates). These variations were not correlated with species (African green monkey, BSC40 and CV-1; human, HeLa and A549), tissue of origin (kidney, BSC40 and CV-1; lung, A549; cervical, HeLa) or oncogenicity.

(ii) Expression profile of viral proteins. We also monitored the expression profile of representative early and late proteins in these infected cells by immunoblot analysis and observed striking and unexpected differences (Fig. 4B). In BSC40 cells, the accumulation of the late proteins L4 and F17 during vΔI3 infections was equivalent or higher than that seen during WT infections, although the reduction in viral yield was the greatest. HeLa cells were the next most permissive for late protein accumulation. A549 cells weakly expressed late proteins, and only trace amounts of late proteins were observed in CV1-CAT cells (as had been shown above).

(iii) DNA accumulation profile. In CV1-CAT cells, as described above, no viral DNA accumulation was observed during vΔI3 infection (<0.2%). To explore whether the gradient in late protein accumulation was due to a gradient in DNA synthesis, we infected each of these cell lines with WT virus or vΔI3 and harvested cells at 10 hpi for analysis by Southern dot blot hybridization and PFGE. A quantitative assessment of the accumulation of bulk viral DNA by Southern dot blot hybridization is shown in Fig. 5A. For BSC40, HeLa, A549, and CV1-CAT cells, viral DNA accumulation during vΔI3 infections was approximately 5, 12.5, 2.2, and 1.2% of that seen with WT virus, respectively. These quantitative data were complemented by a qualitative assessment of the DNA that accumulated during infection (Fig. 5B). Monomeric genomes of 195 kb (arrow) were clearly seen in all samples from WT-infected cells. In BSC40 and HeLa cells infected with vΔI3, no full-length genomes were observed, but there was evident accumulation of subgenomic viral DNA (bracket), with the size distribution ranging from ~25 to 75 kb in BSC40 cells and somewhat larger than that in HeLa cells. In contrast, no viral DNA was detected in samples prepared from A549 or CV1-CAT cells infected with vΔI3.

The increased levels of viral DNA that accumulated in BSC40 and HeLa cells, albeit subgenomic, correlated with the levels of late proteins that were observed. These data indicate that substantial expression of late viral proteins can occur when the levels of DNA that accumulate are ≥5% of WT levels and that subgenomic DNA is sufficient for late gene expression. To ensure that these data (obtained at 10 hpi) were reflective of what was occurring throughout infection, we performed a time course experiment in both BSC40 cells (more permissive for genome replication) and CV1-CAT cells (most restrictive for genome replication) and harvested samples for PFGE analysis at 4, 6, 8, 10, and 24 hpi. These data are shown in Fig. 5C. The typical time course of viral DNA synthesis was seen in all cells infected with WT virus. In BSC40 cells infected with vΔI3

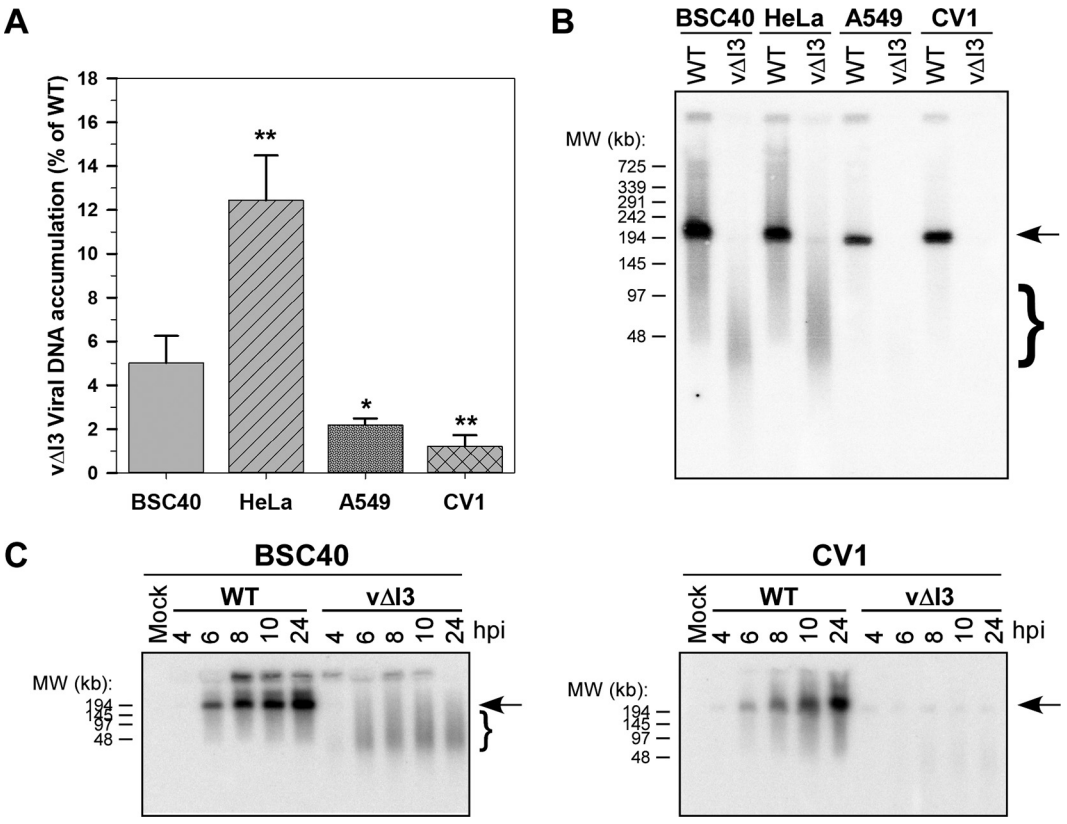

FIG 5 In the absence of I3, DNA accumulation varies among different cell lines. (A and B) Loss of full-length DNA and accumulation of subgenomic DNA in BSC40 and HeLa cells in the absence of I3. BSC40, HeLa, A549, and CV1-CAT cells were infected with WT virus or vΔI3 (MOI, 5) for 10 h; samples were processed for Southern dot blot analysis (A) or PFGE followed by Southern blotting (B). (A) Data are plotted as the average from four experiments and represent the amount of bulk viral DNA accumulated during vΔI3 infections as a percentage of DNA synthesized during WT infections. Error bars represent standard error of the mean (*, $P < 0.05$; **, $P < 0.02$). (B) A representative image of a Southern blot/PFGE analysis is shown; the arrow represents accumulation of full-length genome, and the bracket represents subgenomic viral DNA. (C) Subgenomic DNA is observed throughout infection in BSC40 cells. BSC40 cells (left panel) or CV1-CAT cells (right panel) were infected with WT virus or vΔI3 (MOI, 5). Samples were harvested at the indicated time points (4 to 24 hpi) and processed for PFGE followed by Southern blotting. A representative image is shown; the arrow represents accumulation of full-length genome, and the bracket represents subgenomic viral DNA.

virus (left panel), subgenomic DNA fragments were observed once again and appeared to be present at equivalent levels from 6 to 24 hpi. In CV1-CAT cells infected with vΔI3 (right panel), no viral DNA was observed at any time point. These data confirm the phenotype shown in Fig. 5B and underscore the finding that there are qualitative and quantitative, rather than temporal, differences in the profiles of DNA synthesis in the two cell lines.

(iv) Visualization of virion morphogenesis in BSC40 cells infected with WT virus or vΔI3 by electron microscopy. In BSC40 cells infected with vΔI3, the viral yield is reduced by ~1,500-fold (relative to WT virus infection), although subgenomic DNA accumulates to ~5% of WT levels and late proteins accumulate to near WT levels. We postulated that this dramatic loss of viral yield would reflect a defect in virion morphogenesis due the absence of full-length progeny genomes. We therefore examined BSC40 cells infected with WT virus or vΔI3 at 18 hpi by transmission electron microscopy. As shown in Fig. 6A (and at a higher magnification in Fig. 6B), all the hallmarks of normal morphogenesis were seen in WT-infected cells: crescents (C), immature virions (IV), immature virions with nucleoids (IVN), and numerous clusters of mature virions (MV). In vΔI3-infected cells (Fig. 6C and, at a higher magnification, D), although crescents and immature virions were seen in large numbers, no immature virions with nucleoids or mature virions were observed. Instead, spherical structures of smaller size

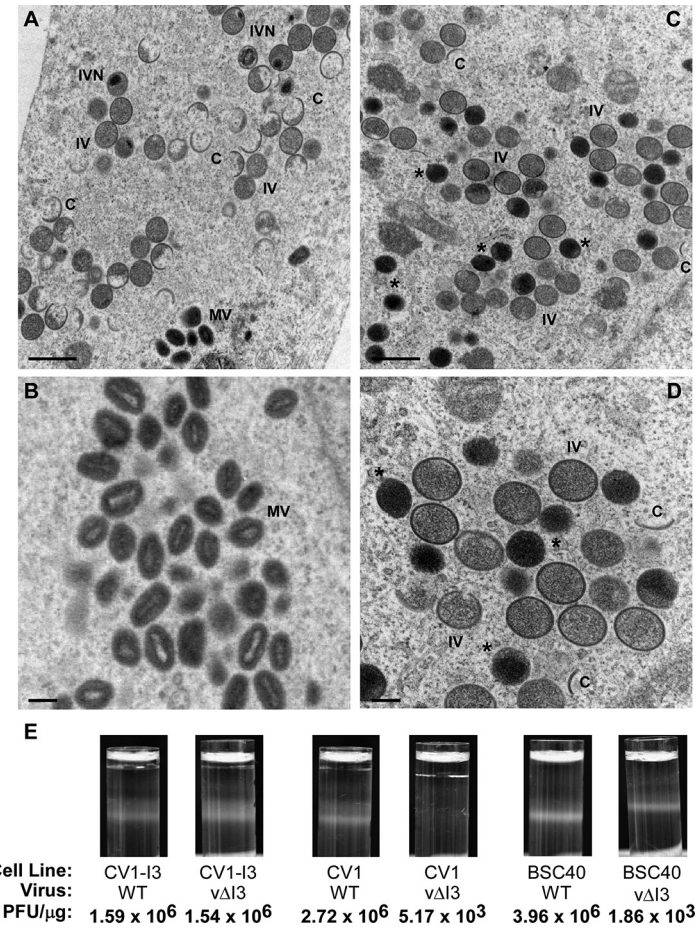

FIG 6 Production of mature and infectious virions is blocked during vΔI3 infection. (A to D) Electron microscopy reveals a specific block in virion assembly when I3 is absent. BSC40 cells were infected with WT virus (A and B) or vΔI3 (C and D) (MOI, 5) for 18 h and processed for electron microscopy. Representative images are shown. C, crescent membrane; IV, immature virion; IVN, immature virion with nucleoid; MV, mature virion; *, aberrant virion. Scale bars, 600 nm (A and C) and 200 nm (B and D). (E) Production of infectious virions is severely diminished in the absence of I3. Preinduced CV1-I3, CV1-CAT, and BSC40 cells were infected with WT or vΔI3 virus (MOI, 5) for 18 h. Virions were purified and light-scattering bands were photographed. Comparable volumes of material from each gradient were retrieved by needle aspiration and concentrated by ultracentrifugation. Total protein and viral titer were determined; specific infectivity is reported as PFU per microgram of protein.

and greater electron density than immature virions, and lacking any internal structure, were observed (*). Such aberrant virions have been seen before when DNA encapsidation was blocked by the repression of the A32 protein (30) or the impairment of the telomere binding protein I6 (31). These images support the conclusion that, although late proteins are abundant during vΔI3 infections of BSC40 cells, infectious virions are not produced because the viral DNA that does accumulate (5% of WT levels) is subgenomic and cannot be encapsidated.

(v) Purification and quantification of virions and specific infectivity. As a complement to the electron microscopy data described above and to provide a more quantitative assessment of mature virion production, BSC40 cells, CV1-CAT cells (negative control), and induced CV1-I3 cells (positive control) were infected with WT virus or vΔI3 (MOI of 5, 18 hpi), and progeny virions were purified on sucrose gradients. Mature virions, but not immature virions, produce light-scattering bands under these conditions. Moreover, the "aberrant virions" that have initiated maturation but are devoid of DNA have previously been shown to form light-scattering bands (31). Images of the sucrose gradients after ultracentrifugation are shown in Fig. 6E. In complementing CV1-I3 cells, light-scattering bands were seen in samples harvested from both WT

virus and vΔI3. In CV1-CAT cells, the WT infection produced a light-scattering band, but no band was seen in the sample harvested from the vΔI3 sample, consistent with the lack of DNA replication and lack of late protein expression. In BSC40 cells, the vΔI3 infection did yield a light-scattering band, and its migration was slightly but detectably different from that seen after a WT infection. After needle aspiration of the light-scattering band and concentration of the virions by ultracentrifugation, the amount of protein was quantified and the infectivity determined. The calculated PFU per microgram of protein for all 6 preparations is shown in Fig. 6E. The relative specific infectivities of the WT versus vΔI3 preparations in the three cell lines were as follows: CV1-I3, 1; CV1-CAT, 526; and BSC40, 2,129. Clearly, the aberrant virions produced during vΔI3 infections of BSC40 cells are not infectious, as predicted.

Utilization of complementing cell lines for structure-function analysis of I3. The successful isolation of vΔI3 was enabled by the ability of I3 expressed from the CV1-I3 cell line to fulfill all of the functions of I3. Traditionally, poxvirology has relied on transient complementation, in which plasmids expressing a variety of alleles of a given viral protein are introduced by transfection and tested for their ability to sustain viral replication. Although powerful, there are limitations to this approach, since not all cells will be transfected and it can be difficult to control the efficiency of transgene expression. The approach used in this study ensures that all cells express the transgene and that the protein of interest is present prior to and throughout infection. We have previously described the use of clustered charge-to-alanine mutagenesis to isolate 10 alleles of I3 for biochemical analysis (13). Three of these mutants (mutants 4, 5, and 7) showed a defect in multimerization *in vitro*. Mutant 5 was the only variant to show a significant decrease in the ability to bind to ssDNA; when electrophoretic mobility shift assay (EMSA) analyses were performed with 30 and 90 ng of protein, the binding of His-tagged I3 mutant 5 to the DNA probe was reduced to 10 and 35% of that seen with the HIS-I3 WT protein, respectively. To further assess whether these alleles could support viral replication, we constructed CV1-I3 cell lines expressing the I3 mutants 4, 5, and 7 and studied the ability of these lines to complement vΔI3. CV1-I3 and CV1-CAT cells were used as the positive and negative controls, respectively.

These cell lines were induced with 50 ng/ml doxycycline and infected with vΔI3 (MOI, 5) for 18 h (Fig. 7A). Infections with vΔI3 produced viral yields that were ~125-fold higher in CV1-I3 WT cells than in CV1-CAT cells (Fig. 7A). The cell lines expressing allele 4 and allele 7 were able to complement vΔI3, albeit at somewhat reduced levels compared to WT I3 (37-fold and 78-fold rescue, respectively). In contrast, the infectious yield was increased only 2-fold in the cell line expressing allele 5. It is important to note that all of the I3 mutant proteins were expressed at nearly equivalent levels (Fig. 7B).These data strongly imply that the ssDNA binding activity of I3 is essential for its role in the viral replication cycle, although we cannot rule out that mutant 5 has additional defects. In addition to monitoring viral yield, we analyzed the profile of viral protein expression. Both early and late viral proteins were expressed to nearly equivalent levels after infection of the CV1-I3, CV1-I3 4, and CV1-I3 7 cells, as would be expected given the high levels of virus produced. As shown above, neither I3 nor viral late proteins were seen in CV1-CAT cells. Surprisingly, however, L4 and, to some extent, F17 accumulated in CV1-I3 5 cells, despite the failure of this cell line to restore the production of infectious virus.

This finding was reminiscent of what we had observed for vΔI3 in BSC40 and HeLa cells, in which late proteins were seen and low levels of subgenomic DNA was observed (Fig. 4 and 5), although the viral yield was greatly reduced. We therefore performed both Southern dot blot and PFGE analyses to monitor DNA accumulation in this panel of CV1-I3-expressing cells infected with vΔI3. As shown in Fig. 7C, the different cell lines supported different levels of DNA replication. As expected, virtually no DNA was seen after infection of CV1-CAT cells. When the cell lines expressing I3 mutants 4, 5, and 7 were infected with vΔI3, the levels of DNA that accumulated were approximately 35, 20, and 60% of that seen in the cells expressing WT I3, respectively. A more qualitative

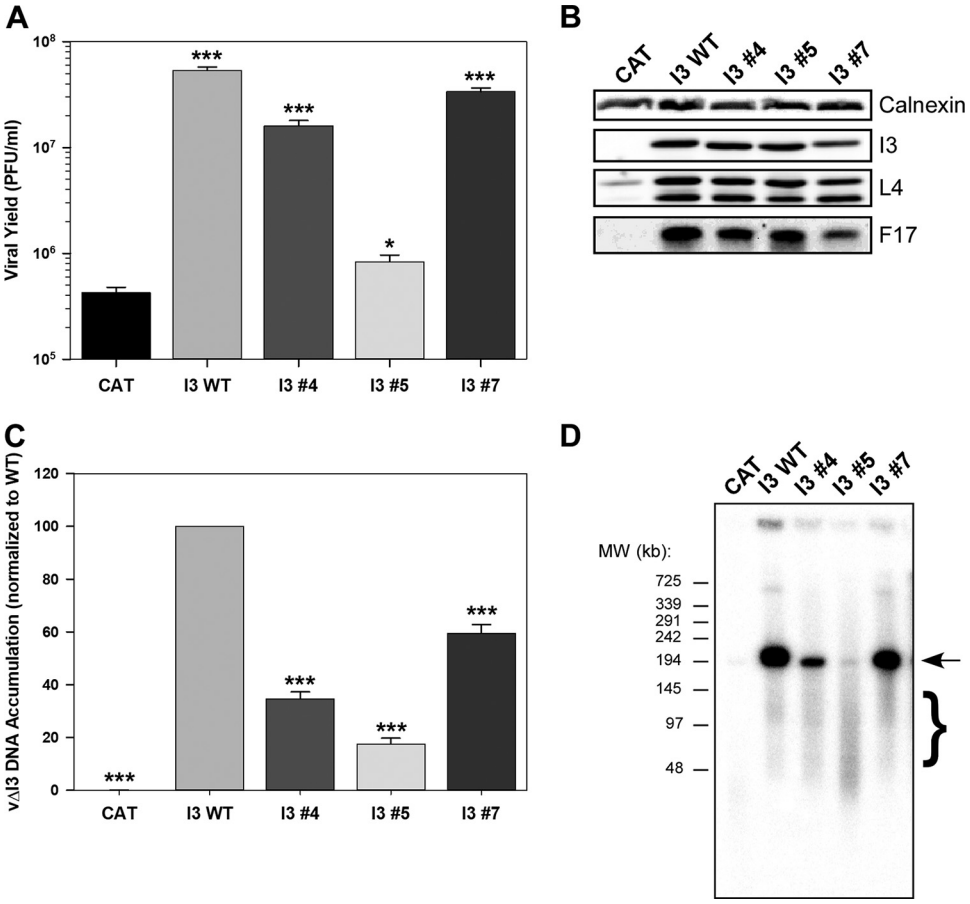

FIG 7 Characterization of vΔI3 infections in CV1 cell lines expressing mutant alleles of I3: ssDNA binding activity is important for complementation. (A) I3 variants with defects in multimerization or ssDNA binding activity differ in their ability to support vΔI3 infection. CV1 cell lines (CAT, WT, 4, 5, and 7) were induced for 24 h with 50 ng/ml doxycycline and then infected with vΔI3 for 18 h. Viral yield is plotted as the average from three experiments. Error bars represent standard error of the mean (*, $P < 0.05$; ***, $P < 0.001$). (B) Late protein accumulation is restored in the presence of various mutant I3 alleles. Infections were performed as for panel A, and cell lysates were processed for immunoblot analysis using antisera directed against calnexin, I3, L4, and F17. A representative blot is shown. (C and D) Quantitative and qualitative defects in viral DNA replication are observed during vΔI3 infections of cell lines expressing I3 variants. CV1 cell lines (CAT, WT, 4, 5, and 7) were induced for 24 h with 50 ng/ml doxycycline. Cells were infected with vΔI3 for 10 h, and cell lysates were processed for Southern dot blot analysis ($n = 3$) (C) and PFGE followed by Southern blotting (representative of $n = 2$) (D). (C) The amount of DNA accumulated during a vΔI3 infection is shown as a percentage of DNA synthesized during a WT infection. Error bars represent standard error of the mean (***, $P < 0.001$). (D) A representative Southern blot is shown; the arrow represents accumulation of full-length genome; and the bracket represents subgenomic viral DNA.

assessment of the DNA that did accumulate was obtained using PFGE, as shown in Fig. 7D. As expected, no signal was seen from CV1-CAT cells. Full-length monomeric DNA was observed in cells expressing WT I3, and a less intense but clear signal was seen in the I3 mutant-4 and I3 mutant-7 cell lines. The relative amounts of the DNA accumulated in the latter two cell lines approximated what had been seen in the dot blots shown in Fig. 7C. In contrast, although a faint signal was seen at the position of monomeric genome in the I3 mutant-5 cells, most of the DNA that accumulated was subgenomic in size. Thus, the significantly reduced ssDNA binding activity of I3 mutant 5 is correlated with both qualitative and quantitative reductions in the accumulation of viral DNA.

DISCUSSION

In this report, we provide definitive confirmation that the I3 protein encoded by vaccinia virus plays an essential role in the viral life cycle. It has been known for many years that I3 has the biochemical properties of a canonical SSB and that it localizes to

viral replication factories. Partial depletion of I3 has been shown to impair DNA replication and recombination (15, 20), but definitive genetic analysis has been lacking. Here we have established a complementing cell line (CV1-I3) carrying an inducible, codon-optimized allele of I3; the levels of I3 that accumulate upon induction are close to those seen during infection with WT virus. With this cell line in hand, we have also generated a deletion mutant that lacks the I3 open reading frame (ORF) (vΔI3) but replicates to wild-type levels in the complementing cell line (Fig. 1).

In a noncomplementing cell line (CV1-CAT) (Fig. 2), early protein expression proceeds normally, and the other proteins involved in DNA replication (A20, E9, D5, and H5) accumulate to WT levels. Moreover, core disassembly, which is a prerequisite for the replication of the viral genome, also proceeds in the absence of I3. During a WT infection, I3 has been found to colocalize with the encapsidated genome upon its release from the core and has been used as a marker of these "prereplication foci" (22). Determination of what other proteins associate with the newly released parental genome is an area for future study, as is the analysis of whether the stability or conformation of the genome is in some way compromised by the absence of I3.

Having shown that many of the replication proteins accumulate normally in the absence of I3 and that core disassembly occurred, the next step for analysis was the synthesis of progeny genomes (Fig. 3A and B). We utilized Southern dot blot hybridization and PFGE to assess DNA accumulation both quantitatively and qualitatively from 4 to 24 hpi: DNA synthesis was essentially absent ($<$0.2% of WT levels). As would be predicted given the absence of DNA replication, the temporal progression of protein synthesis was severely disrupted, with minimal evidence of the transition to late protein synthesis (Fig. 3C). Even when the highly abundant late proteins L4 and F17 were assessed by immunoblot analysis, only trace levels of proteins could be seen (Fig. 3D). By 18 hpi, the yield of infectious virus produced from CV1-CAT cells infected with vΔI3 was reduced by ~350-fold compared to that for WT infections performed in parallel (Fig. 1E).

As another measure of the importance of I3 to viral infection, we performed plaque assays on induced CV1-CAT and CV1-I3 cells. vΔI3 was unable to form macroscopic plaques on noncomplementing cells, although it formed plaques of WT size on the complementing CV1-I3 cells (Fig. 1D). We also measured the viral yield after WT and vΔI3 infections of CV1-CAT, A549, BSC40, and HeLa cells (Fig. 4A). In each cell line, vΔI3 was severely defective (168- to 1,776-fold reduction). For the sake of completeness, we also monitored DNA accumulation and late protein accumulation in each cell line, and were surprised to see significant levels of late proteins in both BSC40 and HeLa cells (Fig. 4B). Moreover, these cell lines accumulated 5 and 12.5% of WT levels of viral DNA, respectively (Fig. 5A), although all of the DNA that accumulated was subgenomic in size. (Fig. 5B). These data were unexpected. It is interesting to note that this subgenomic DNA was first seen in vΔI3 infections by 6 hpi, similar to the time at which full-length genomes are seen by PFGE during a WT infection. However, no further increase in the amount of DNA was seen as the infection progressed (Fig. 5C). It is possible that the subgenomic DNA is a poor template for further rounds of synthesis or that it is relatively unstable.

Why would the severity of the DNA replication phenotype of vΔI3 show cell type variations, and why would the DNA that was synthesized be subgenomic in size? SSBs are a central component of all prokaryotic and eukaryotic replication systems that have been studied, and two core requirements have been posited (32, 33). DNA replication requires that the two strands of the dsDNA template be separated, but ssDNA is less energetically favorable than dsDNA. Therefore, the ssDNA tends to form intramolecular regions of dsDNA, which occlude further enzymatic transactions. SSBs keep the DNA unfolded and in a single-stranded state. Second, ssDNA is highly susceptible to attack by nucleases, and coating by SSBs is protective. I3 is likely to perform both of these functions during viral DNA replication in all cell lines infected. Might the levels of cytoplasmic nucleases be lower in BSC40 and HeLa cells than in CV1-CAT and A549 cells? If so, then any DNA that would be synthesized might be more stable and the

fragments larger in the latter two cell lines. It is also possible that cellular proteins with SSB activity might be more abundant in the cytoplasm of certain cell types and could provide partial complementation. This is an area for future study. Our preliminary data do not show a difference in the levels of cytoplasmic RPA2 (a component of the trimeric replicative SSB RPA) in the different cell lines tested, but we have not tested this exhaustively, nor have we monitored the cytoplasmic levels of SSB1 or SSB2, two additional mammalian SSBs that play roles distinct from those of RPA (32, 34).

SSBs are now appreciated as playing additional roles in most replication systems (33, 34). They are considered to be "hubs" that bring numerous other proteins to DNA that is undergoing replication, repair, and recombination. In many systems, SSBs have charged C′-terminal tails that mediate protein-protein interactions. In the case of I3, no such interactions have been found, and instead the C′-terminal tail has been shown to modulate DNA binding, as has also been shown for some prokaryotic SSBs (16). Another area of study for the future is to assess the repertoire of proteins that I3 might interact with during viral replication. These could include viral or cellular proteins that might participate in processes such as recombination or repair, as has been observed for the herpes simplex virus-encoded SSB ICP8 (35–37).

Vaccinia virus infection is associated with high levels of recombination, and the Evans laboratory has performed extensive analysis of the *cis*- and *trans*-acting factors that contribute to recombination (20, 38, 39). A single-strand annealing mechanism (SSA) rather than a single-strand invasion mechanism (SSI) is favored, with the 3′-5′ exonuclease activity of the E9 polymerase thought to generate 5′ overhangs in a manner that is stimulated by I3. If recombination is an intrinsic part of replication, then the subgenomic fragments seen during vΔI3 infections of BSC40 cells might reflect an inability to assemble full-length genomes from subgenomic intermediates. Interestingly, subgenomic fragments are also characteristic of infections with a virus lacking the G5 protein (11; Czarnecki and Traktman, unpublished), which has significant homology to the FEN-1 family of nucleases. Examination of physical or functional interactions between I3 and G5 is another area for future study.

As was seen in the study of the G5 deletion virus, we observed that BSC40 and HeLa cells infected with vΔI3 accumulated late proteins at nearly WT levels. These data indicate that synthesis of as little as 5% of WT levels of viral DNA is sufficient for the transcription and synthesis of late proteins. Moreover, these data also indicate that subgenomic fragments are competent for late transcription. The Moss laboratory recently published a study using the iPOND (isolation of proteins on nascent DNA) technique to retrieve proteins bound to nascent DNA after a 20-min pulse with 5-ethynyl-2′-deoxyuridine (EdU) (40). They found that in addition to retrieving the components of the replication machinery, they also retrieved proteins involved in both intermediate and late transcription. These data suggest that transcription may be occurring on the same genomes that are undergoing replication, consistent with our finding that subgenomic DNA is competent for transcription.

Interestingly, as would be predicted from the accumulation of late proteins, BSC40 cells infected with vΔI3 had high levels of intermediates in virion morphogenesis, such as virosomes, crescents, and immature virions. However, no immature virions with nucleoids were seen, suggesting that genome encapsidation was not occurring. Similarly, no mature virions were seen. However, numerous aberrant virions that closely resembled those seen during *ts*I6 infections and A32-deficient infections were seen (30, 31). I6 is a telomere binding protein that associates with the hairpin telomeres of the monomeric viral genome (41), and A32 is thought to be a pumping ATPase of the FTS-HerA family (42, 43). When I6 is defective or A32 is absent, viral genomes are not encapsidated (30, 31). These spherical, electron-dense, aberrant virions lack DNA, have no visible internal structure, and are not infectious. Interestingly, however, BSC40 cells infected with vΔI3 do not contain the crystalloids seen when I6, A32, or the viral A13 protein is defective or absent (30, 31, 44). These electron-dense crystalloids contain closely packed arrays of viral DNA. Our failure to detect crystalloids in the vΔI3-infected BSC40 cells might reflect the low levels of DNA that accumulate in BSC40 cells infected

with vΔI3 (~5% of WT level) or might reflect the need for the full 195-kb genome with the structured telomeres for crystalloid formation.

As mentioned in the introduction, I3 is an atypical SSB, lacking any obvious OB fold and showing no sequence homology to other viral or cellular SSBs (15, 17). Homology to the prokaryotic family of tmRNA binding proteins has recently been proposed (17). With the genetic tools that we have developed, we are now in a position to perform structure-function analysis of I3 both *in vitro* and *in vivo*. In an earlier study, we generated 10 mutant alleles of I3 and subjected proteins encoded by these alleles to biochemical analysis. Using *in vitro* transcription/translation to generate proteins, mutants 4, 5, and 7 were found to be defective in I3-I3 interactions *in vitro*. We also purified recombinant proteins after expression in *E. coli* and found that mutant 5 showed a striking and significant defect in ssDNA binding. In the current study, we generated CV1-I3 cell lines carrying each of these 3 mutant alleles.

Mutants 4 and 7 showed a moderate but significant diminution in their ability to complement vΔI3 and to support viral DNA replication. Perhaps I3-I3 interactions are less crucial *in vivo* than might have been expected, or perhaps these interactions are augmented by posttranslational modification or interactions with other proteins. Mutant 5, in contrast, was unable to mediate any significant rescue of vΔI3 infection, despite accumulating to levels comparable to those of the WT protein. The lack of complementation was associated with diminished accumulation of viral DNA, most of which was subgenomic in size. This phenotype is similar to that seen in BSC40 cells infected with vΔI3, and unraveling the mechanism underlying the formation of subgenomic DNA is of significant interest. These important data underscore that I3's ssDNA binding activity is essential for its biological function. Our newly developed genetic system will allow us to assess the impact of phosphorylation on I3's function, as well as to test the impact of mutagenizing other conserved residues and domains on its ability to support the viral life cycle. There is much to be learned about how I3, an atypical SSB, supports the replication, recombination, and repair of the vaccinia virus genome.

MATERIALS AND METHODS

Reagents. The Flp-In system, Lipofectamine 2000, blasticidin, hygromycin, zeocin, and Alexa Fluor 488 goat anti-rabbit (GAR) IgG were purchased from Life Technologies (Grand Island, NY). Doxycycline was purchased from Sigma (St. Louis, MO). A codon-optimized I3 (coI3) ORF was synthesized by GeneArt Gene Synthesis (now part of Life Technologies). Paraformaldehyde (PFA) was purchased from Electron Microscopy Sciences (Hatfield, PA). Zeta Probe blotting membranes were purchased from Bio-Rad (Hercules, CA), and protran nitrocellulose membranes were obtained from GE Healthcare Life Sciences (Buckinghamshire, UK). [^{32}P]dATP and [^{32}P]TTP were purchased from PerkinElmer Life Sciences (Boston, MA). Oligonucleotide primers were purchased from Integrated DNA Technologies (Coralville, IA). Restriction endonucleases, T4 DNA ligase, calf intestinal phosphatase (CIP), pancreatic RNase, PCR-grade deoxynucleoside triphosphates (dNTPs), *Taq* DNA polymerase, and DNA molecular weight standards were purchased from Roche Diagnostics (Indianapolis, IN) and were used per the manufacturer's specifications. Proteinase K was purchased from Sigma-Aldrich (St. Louis, MO), and SeaKem LE agarose was purchased from Lonza Inc. (Allendale, NJ). Molecular weight standards for pulsed-field gel electrophoresis, including Lambda PFGE marker and Quick-Load 1-kb extended DNA ladder, were purchased from New England BioLabs Inc. (Ipswich, MA).

Cells and virus. African green monkey BSC40 cells were maintained at 37°C in Dulbecco modified Eagle medium (DMEM) (Life Technologies) containing 5% fetal calf serum (FCS). A549 cells (ATCC CCL-185) and HeLa cells (ATCC CCL-2.2) were maintained at 37°C in DMEM containing 10% FCS. Flp-In-CV1 fibroblast cells were obtained from Life Technologies and maintained in DMEM containing 10% FCS; the Flp-In-CV1-TetR cells, expressing the TET repressor, were generated in our laboratory (10). The control CV1-CAT cells, expressing a doxycycline-inducible chloramphenicol acetyltransferase protein, and the experimental CV1-I3 cells, expressing a doxycycline-inducible codon-optimized I3 protein, were generated in our laboratory (see below). For induced conditions, 50 ng/ml doxycycline was added 24 h prior to infection.

The vΔI3 virus, whose generation is described below, was propagated in the CV1-I3 cells in the presence of 50 ng/ml doxycycline. Viral stocks were prepared by ultracentrifugation of cytoplasmic lysates through 36% sucrose; titers were determined by plaque assays performed on preinduced CV1-I3 cells.

Construction of the CV1-I3 stable cell line. The I3 ORF was codon optimized for expression in mammalian cells by GeneArt (Regensburg, Germany) and cloned into pcDNA5/FRT/TO (Life Technologies) using the HindIII and BamHI restriction sites. Flp-In-CV1-TetR cells (10) were cotransfected with pcDNA/FRT/TO-I3 and pOG44, a plasmid containing the *Saccharomyces cerevisiae* Flp recombinase, using Lipofectamine 2000 per the manufacturer's instructions. Recombinational integration of the I3 ORF into

TABLE 1 Primers used in this study

Name	Sequence (5′→3′)[a]
Upstream primers (sense strand)	
U-4,5,7	GC**AAGCTT**GGAGGAGCCACC
4_C	GCCTGTCCGCGGCAGCGGCGCAGCTGGCCAAGGCC
5_C	CGCCCTGGCGGCGCTGATCATCGACCGC
7_C	GCGATAGCGCGGCGGTGTCCATGACCGAG
U-I3 KO	GCC**AAGCTT**TCAATGCAC
I3 KO_C	CTC**GTCGACCTCGAGCATATG**GATTAA ACCTAAATAATT
Downstream primers (antisense strand)	
D-4,5,7	GC**GGATCC***TCA*GACGTTGAAG
4_B	GCCAGCTGCGCCGCTGCCGCGGACAGGCTTTCCAG
5_B	GATGATCAGCGCCGCCAGGGCGAAGGTGATC
7_B	CATGGACACCGCCGCGCTATCGCCAGACAG
D-I3 KO	CTC**GGTACC**CAGAAGATATTAAGCG
I3 KO_B	CTC**GTCGAC**ATGATGAAGATAGCG

[a]Restriction enzyme sites are in bold, the altered nucleotides are underlined, and the terminating codon is in italic. For overlap PCRs, U(x) + X_B and D(x) + X_C.

the single FLP recombination target (FRT) site present in the parental cell line places it under the regulation of the cytomegalovirus (CMV) promoter and two tandem copies of the TET operator. Integration of the I3-expressing plasmid was selected for by growth in medium containing 75 μg/ml hygromycin and 30 μg/ml blasticidin to obtain pure populations of cells. Properly targeted cells were validated by immunoblot analysis. In parallel, a CV1-CAT cell line containing a single, inducible transgene encoding chloramphenicol acetyltransferase (CAT) was generated as a control.

Construction of an I3 deletion mutant (vΔI3). (i) Generation of the targeting plasmid. The vΔI3 targeting construct was designed such that the vast majority of the I3L ORF was deleted and replaced with RFP. The left-hand flanking sequence of the construct (336 bp) contained the C-terminal 66 bp of the I1 ORF, the short I1-I2 intergenic region, the I2 ORF, and the stop codon and the last 44 bp from the C′ terminus of the I3L ORF. The latter region was retained to ensure that the I2L promoter, which is embedded within the C′ terminus of the I3 ORF, remained intact. The right-hand flanking sequence (387 bp) contained the 82-bp I3L-I4L intergenic region, which contains the I3L promoter, and 305 bp from the C′ terminus of I4L. Insertion of the RFP ORF between these two flanking regions places RFP under the regulation of the endogenous I3 promoter.

The left-hand flank was amplified from the viral genome using primers U-I3 KO and I3 KO_B (all primers are shown in Table 1), which insert HindIII and SalI sites at the termini of the PCR product, respectively. The right-hand flank was amplified from the genome using primers I3 KO_C and D-I3 KO, which insert SalI, XhoI, and NdeI sites and an Asp.718 site at the termini of the PCR product, respectively. The left-hand flanking PCR product was digested with HindIII and SalI and the right-hand flanking product with SalI and Asp.718, and they were together ligated to a pBSIIKS vector that had been digested with HindIII and Asp.718 and treated with calf intestinal alkaline phosphatase. Once this intermediate plasmid was generated and validated by DNA sequencing, it was digested with NdeI and XhoI and ligated to an NdeI-XhoI fragment carrying the RFP ORF. The final plasmid (pΔI3:RFP) was again validated by restriction enzyme digestion and DNA sequencing.

(ii) Recombinational targeting of the endogenous I3 genomic locus to generate the vΔI3 virus. BSC40 cells were infected with WT virus (MOI, 3) and transfected with linearized pΔI3:RFP DNA at 3 hpi. Cells were harvested at 24 hpi, and RFP-expressing virus was isolated by iterative plaque purification on complementing CV1–I3 cells (preinduced with 50 ng/ml doxycycline). Iterative rounds of plaque purification were performed under conditions of limiting dilution (≤1 plaque/well) until all of the subsequent progeny plaques expressed RFP, as visualized by live immunofluorescence microscopy. The replacement of the I3 ORF with RFP and the purity of the viral stock were confirmed by PCR (not shown) and immunoblot analysis. The resulting virus was named vΔI3.

Determination of infectious viral yield from a single cycle of infection. CV1-CAT (with or without DOX), CV1-I3 (with or without DOX), BSC40, HeLa, or A549 cells were infected with WT virus or vΔI3 (MOI, 5) and harvested at 18 hpi. Cells were collected by centrifugation, resuspended in 1 mM Tris (pH 9.0), and disrupted by freeze-thawing and sonication. Viral yields were assessed in plaque assays performed under permissive conditions (CV1-I3 with DOX). The viral yield was plotted as the average from three experiments with error bars representing the standard error of the mean. A Student one-tailed *t* test was employed to determine significance.

Plaque assay. Confluent monolayers of CV1-CAT or CV1-I3 cells were induced with 50 ng/ml doxycycline for 24 h. Cells were then infected with 50 plaques of WT or vΔI3 virus. Cells were incubated for 48 h at 37°C and stained with crystal violet.

Southern dot blot hybridization to assess bulk viral DNA accumulation. The indicated cell lines were left uninfected or infected with WT virus or vΔI3 (MOI, 5) and harvested at the time points indicated (10 hpi for single-point experiments and 4, 6, 8, 10, and 24 hpi for time courses). Samples were prepared as described previously (45) and spotted in triplicate on Zeta Probe membranes. Membranes were

hybridized with ^{32}P-labeled probes representing fragments of the vaccinia virus genome (prepared by nick translation). Data were obtained by phosphorimager analysis (Typhoon FLA-9000) and quantified using ImageQuantTL software.

PFGE. The indicated cell lines were left uninfected or infected with WT virus or vΔI3 (MOI, 5) and harvested at 10 hpi (for single-point experiments) or 4, 6, 8, 10, and 24 hpi (for time course experiments). Washed cell pellets were processed as previously detailed (15). DNA was resolved on a CHEF Mapper XA apparatus (Bio-Rad) using one of two sets of parameters: (i) 6 V/cm for 12 h at 14°C, using a switching time gradient of 1 to 25 s, a linear ramping factor, and a 120° angle (this program resolved DNA species of 2 to 750 kb), or (ii) 6 V/cm for 5 h at 14°C, using a switching time gradient of 0.05 to 17 s, a ramping factor of 2.84, and a switching angle of 120° (this program resolved DNA species of 0.2 to 500 kb). DNA was visualized by ethidium bromide (EtBr) staining and images captured using the FluorChem E documentation system (ProteinSimple, Santa Clara, CA). Gels were also transferred to Zeta-Probe GT membranes (Bio-Rad) for Southern blot analysis; viral DNA was detected following hybridization with a ^{32}P-labeled probe as described above for Southern dot blot analysis.

Immunoblot analysis of viral and cellular protein accumulation. Whole-cell lysates were prepared, resolved on SDS-acrylamide gels, and transferred electrophoretically to nitrocellulose membranes. For quantification of I3 accumulation, the protein concentration was determined using the bicinchoninic acid (BCA) protein assay kit (Thermo Fisher), and 50 μg of total protein was resolved. The membranes were probed with antisera directed against the following viral proteins: E9 (46), A20 (47), D5 (48), I3 (13), H5 (24), L4 (49), G7 (50), and F17 (49). Calnexin was used as a loading control and was detected using an anticalnexin antibody (ADI-SPA-860-F; Enzo Life Sciences, Farmingdale NY). The immunoreactive proteins were detected using horseradish peroxidase-conjugated secondary antisera (Bio-Rad) and chemiluminescent SuperSignal West Pico reagents (Pierce, Rockford, IL). Immunoreactive proteins were visualized by exposure on a FluorChem E documentation system (ProteinSimple, Santa Clara, CA) and quantified using AlphaView software (ProteinSimple).

Immunofluorescence assays. For I3 localization, CV1-I3 cells were left untreated or treated with doxycycline (50 ng/ml) for 18 h. For the uncoating assay, CV1 cells were infected (MOI, 15) in the absence or presence of cycloheximide (25 μg/ml) or araC (20 μM). At 3 hpi, cells were fixed in 4% (vol/vol) PFA in phosphate-buffered saline (PBS) for 15 min on ice. Following fixation, all samples were washed twice with cold PBS and permeabilized with 0.2% Triton X-100 for 10 min at room temperature. For both I3 localization and the uncoating assay, cells were stained with either an anti-I3 antibody (13) or an anti-A5 antibody (44), followed by visualization with an Alexa Fluor 488 GAR secondary antibody. DAPI (4′,6′-diamidino-2-phenylindole) was added and left for 15 min at room temperature. Samples were mounted with Vectashield (Vector Laboratories, Inc., Burlingame CA), and pictures were captured using a Nikon Eclipse Ti microscope and NIS Elements AR4.4 software (Tokyo, Japan). Scale bars represent 50 nm.

Electron microscopy. Confluent 60-mm dishes of BSC40 cells were infected with WT virus or vΔI3 at an MOI of 5 for 18 h. Samples were washed with Sorensen's buffer and fixed *in situ* with 1% glutaraldehyde in Sorensen's buffer for 30 min at room temperature. Cells were collected by centrifugation at 800 $\times$ *g* for 7 min, and fresh fixative was added. Cells were then processed for conventional electron microscopy and embedded in Embed 810 resin (Electron Microscopy Sciences, Hatfield, PA). Thin sections were examined on a JEOL JEM-1010 microscope, and images were taken using a Hamamatsu camera.

Virion purification. BSC40, CV1-CAT (with DOX), or CVI-I3 (with DOX) cells were infected with WT virus or vΔI3 (MOI of 5, two 15-cm dishes per infection). At 18 hpi, virions were purified by ultracentrifugation through a 36% sucrose cushion followed by a 25 to 40% sucrose gradient. Light-scattering bands were photographed and then retrieved by needle aspiration. Virions were solubilized in a buffer containing 0.25% NP-40, 0.25% deoxycholate, 250 mM NaCl, and 0.5 mM dithiothreitol. Total protein was quantitated using the BCA protein assay kit (Thermo Fisher), and the infectious titer was determined by plaque assay on preinduced CV1-I3 cells.

Analysis of I3 mutant cell lines. Utilizing pcDNA5/FRT/TO coI3 as a template, previously described mutants of I3 (15) were generated using an overlap PCR strategy (primers are shown in Table 1). These plasmids were used to generate pure mutant cell populations as described above. Confluent monolayers of cells were induced with 50 ng/ml doxycycline for 24 h and infected with vΔI3 (MOI 5) for 18 h (for viral yield and protein analysis) or for 10 h (for Southern dot blotting and PFGE). Samples were analyzed for viral yield, DNA, and protein accumulation as described above.

Preparation of digital figures. Images from immunoblot analysis and EtBr-stained gels were acquired using a FluorChem E documentation system (ProteinSimple, Santa Clara, CA); images for the Southern dot blot and Southern blot analyses were acquired on an FLA-9000 Typhoon phosphorimager (GE Healthcare Bio-Sciences, Pittsburgh, PA). Statistical analysis and graph preparation were performed using SigmaPlot software (Systat Software, Chicago, IL). Final figures were assembled and labeled with Canvas software (Deneba Systems, Miami, FL).

ACKNOWLEDGMENTS

We acknowledge the support of NIH grant RO1 AI61758 (awarded to P.T. by NIAID).

We thank Nancy Smythe for help with the electron microscopy and Kathy Boyle for invaluable intellectual and experimental input. Many past and present members of the Traktman laboratory have contributed to this work in helpful ways.

REFERENCES

1. Moss B. 2013. Poxviridae, p 2129–59. *In* Knipe DM, Howley PM (ed), Fields virology, 6th ed, vol 2. Lippincott Williams & Wilkins, Philadelphia, PA.
2. Boyle K, Traktman P. 2009. Poxviruses, p 225–247. *In* Cameron CE, Gotte M, Raney KD (ed), Viral genome replication. Springer, New York, NY.
3. Moss B. 2013. Poxvirus DNA replication. Cold Spring Harb Perspect Biol 5:a010199. https://doi.org/10.1101/cshperspect.a010199.
4. Stanitsa ES, Arps L, Traktman P. 2006. Vaccinia virus uracil DNA glycosylase interacts with the A20 protein to form a heterodimeric processivity factor for the viral DNA polymerase. J Biol Chem 281:3439–3451. https://doi.org/10.1074/jbc.M511239200.
5. Boyle KA, Stanitsa ES, Greseth MD, Lindgren JK, Traktman P. 2011. Evaluation of the role of the vaccinia virus uracil DNA glycosylase and A20 proteins as intrinsic components of the DNA polymerase holoenzyme. J Biol Chem 286:24702–24713. https://doi.org/10.1074/jbc.M111.222216.
6. Boyle KA, Arps L, Traktman P. 2007. Biochemical and genetic analysis of the vaccinia virus d5 protein: multimerization-dependent ATPase activity is required to support viral DNA replication. J Virol 81:844–859. https://doi.org/10.1128/JVI.02217-06.
7. De Silva FS, Lewis W, Berglund P, Koonin EV, Moss B. 2007. Poxvirus DNA primase. Proc Natl Acad Sci U S A 104:18724–18729. https://doi.org/10.1073/pnas.0709276104.
8. Kay NE, Bainbridge TW, Condit RC, Bubb MR, Judd RE, Venkatakrishnan B, McKenna R, D'Costa SM. 2013. Biochemical and biophysical properties of a putative hub protein expressed by vaccinia virus. J Biol Chem 288:11470–11481. https://doi.org/10.1074/jbc.M112.442012.
9. D'Costa SM, Bainbridge TW, Kato SE, Prins C, Kelley K, Condit RC. 2010. Vaccinia H5 is a multifunctional protein involved in viral DNA replication, postreplicative gene transcription, and virion morphogenesis. Virology 401:49–60. https://doi.org/10.1016/j.virol.2010.01.020.
10. Boyle KA, Greseth MD, Traktman P. 2015. Genetic confirmation that the H5 protein is required for vaccinia virus DNA replication. J Virol 89:6312–6327. https://doi.org/10.1128/JVI.00445-15.
11. Senkevich TG, Koonin EV, Moss B. 2009. Predicted poxvirus FEN1-like nuclease required for homologous recombination, double-strand break repair and full-size genome formation. Proc Natl Acad Sci U S A 106:17921–17926. https://doi.org/10.1073/pnas.0909529106.
12. Paran N, De Silva FS, Senkevich TG, Moss B. 2009. Cellular DNA ligase I is recruited to cytoplasmic vaccinia virus factories and masks the role of the vaccinia ligase in viral DNA replication. Cell Host Microbe 6:563–569. https://doi.org/10.1016/j.chom.2009.11.005.
13. Rochester SC, Traktman P. 1998. Characterization of the single-stranded DNA binding protein encoded by the vaccinia virus I3 gene. J Virol 72:2917–2926.
14. Tseng M, Palaniyar N, Zhang W, Evans DH. 1999. DNA binding and aggregation properties of the vaccinia virus I3L gene product. J Biol Chem 274:21637–21644. https://doi.org/10.1074/jbc.274.31.21637.
15. Greseth MD, Boyle KA, Bluma MS, Unger B, Wiebe MS, Soares-Martins JA, Wickramasekera NT, Wahlberg J, Traktman P. 2012. Molecular genetic and biochemical characterization of the vaccinia virus I3 protein, the replicative single-stranded DNA binding protein. J Virol 86:6197–6209. https://doi.org/10.1128/JVI.00206-12.
16. Harrison ML, Desaulniers MA, Noyce RS, Evans DH. 2016. The acidic C-terminus of vaccinia virus I3 single-strand binding protein promotes proper assembly of DNA-protein complexes. Virology 489:212–222. https://doi.org/10.1016/j.virol.2015.12.020.
17. Kazlauskas D, Venclovas C. 2012. Two distinct SSB protein families in nucleo-cytoplasmic large DNA viruses. Bioinformatics 28:3186–3190. https://doi.org/10.1093/bioinformatics/bts626.
18. Welsch S, Doglio L, Schleich S, Krijnse LJ. 2003. The vaccinia virus I3L gene product is localized to a complex endoplasmic reticulum-associated structure that contains the viral parental DNA. J Virol 77:6014–6028. https://doi.org/10.1128/JVI.77.10.6014-6028.2003.
19. Kato SE, Moussatche N, D'Costa SM, Bainbridge TW, Prins C, Strahl AL, Shatzer AN, Brinker AJ, Kay NE, Condit RC. 2008. Marker rescue mapping of the combined Condit/Dales collection of temperature-sensitive vaccinia virus mutants. Virology 375:213–222. https://doi.org/10.1016/j.virol.2008.01.027.
20. Gammon DB, Evans DH. 2009. The 3′-to-5′ exonuclease activity of vaccinia virus DNA polymerase is essential and plays a role in promoting virus genetic recombination. J Virol 83:4236–4250. https://doi.org/10.1128/JVI.02255-08.
21. Kilcher S, Schmidt FI, Schneider C, Kopf M, Helenius A, Mercer J. 2014. siRNA screen of early poxvirus genes identifies the AAA+ ATPase D5 as the virus genome-uncoating factor. Cell Host Microbe 15:103–112. https://doi.org/10.1016/j.chom.2013.12.008.
22. Mercer J, Snijder B, Sacher R, Burkard C, Bleck CK, Stahlberg H, Pelkmans L, Helenius A. 2012. RNAi screening reveals proteasome- and Cullin3-dependent stages in vaccinia virus infection. Cell Rep 2:1036–1047. https://doi.org/10.1016/j.celrep.2012.09.003.
23. Traktman P, Boyle K. 2004. Methods for analysis of poxvirus DNA replication. Methods Mol Biol 269:169–186.
24. McDonald WF, Crozel-Goudot V, Traktman P. 1992. Transient expression of the vaccinia virus DNA polymerase is an intrinsic feature of the early phase of infection and is unlinked to DNA replication and late gene expression. J Virol 66:534–547.
25. Punjabi A, Boyle K, DeMasi J, Grubisha O, Unger B, Khanna M, Traktman P. 2001. Clustered charge-to-alanine mutagenesis of the vaccinia virus A20 gene: temperature-sensitive mutants have a DNA-minus phenotype and are defective in the production of processive DNA polymerase activity. J Virol 75:12308–12318. https://doi.org/10.1128/JVI.75.24.12308-12318.2001.
26. Evans E, Traktman P. 1992. Characterization of vaccinia virus DNA replication mutants with lesions in the D5 gene. Chromosoma 102:S72–S82. https://doi.org/10.1007/BF02451789.
27. DeMasi J, Traktman P. 2000. Clustered charge-to-alanine mutagenesis of the vaccinia virus H5 gene: isolation of a dominant, temperature-sensitive mutant with a profound defect in morphogenesis. J Virol 74:2393–2405. https://doi.org/10.1128/JVI.74.5.2393-2405.2000.
28. Liu K, Lemon B, Traktman P. 1995. The dual-specificity phosphatase encoded by vaccinia virus, VH1, is essential for viral transcription in vivo and in vitro. J Virol 69:7823–7834.
29. Mercer J, Traktman P. 2005. Genetic and cell biological characterization of the vaccinia virus A30 and G7 phosphoproteins. J Virol 79:7146–7161. https://doi.org/10.1128/JVI.79.11.7146-7161.2005.
30. Greseth MD, Carter DM, Terhune SS, Traktman P. 2017. Proteomic screen for cellular targets of the vaccinia virus F10 protein kinase reveals that phosphorylation of mDia regulates stress fiber formation. Mol Cell Proteomics https://doi.org/10.1074/mcp.M116.065003.
31. Condit RC, Moussatche N, Traktman P. 2006. In a nutshell: structure and assembly of the vaccinia virion. Adv Virus Res 66:31–124. https://doi.org/10.1016/S0065-3527(06)66002-8.
32. Wickramasekera NT, Traktman P. 2010. Structure/function analysis of the vaccinia virus F18 phosphoprotein, an abundant core component required for virion maturation and infectivity. J Virol 84:6846–6860. https://doi.org/10.1128/JVI.00399-10.
33. Postigo A, Ramsden AE, Howell M, Way M. 2017. Cytoplasmic ATR activation promotes vaccinia virus genome replication. Cell Rep 19:1022–1032. https://doi.org/10.1016/j.celrep.2017.04.025.
34. Panda D, Fernandez DJ, Lal M, Buehler E, Moss B. 2017. Triad of human cellular proteins, IRF2, FAM111A, and RFC3, restrict replication of orthopoxvirus SPI-1 host-range mutants. Proc Natl Acad Sci U S A 114:3720–3725. https://doi.org/10.1073/pnas.1700678114.
35. Luttge BG, Moyer RW. 2005. Suppressors of a host range mutation in the rabbitpox virus serpin SPI-1 map to proteins essential for viral DNA replication. J Virol 79:9168–9179. https://doi.org/10.1128/JVI.79.14.9168-9179.2005.
36. Cassetti MC, Merchlinsky M, Wolffe EJ, Weisberg AS, Moss B. 1998. DNA packaging mutant: repression of the vaccinia virus A32 gene results in noninfectious, DNA-deficient, spherical, enveloped particles. J Virol 72:5769–5780.
37. Grubisha O, Traktman P. 2003. Genetic analysis of the vaccinia virus I6 telomere-binding protein uncovers a key role in genome encapsidation. J Virol 77:10929–10942. https://doi.org/10.1128/JVI.77.20.10929-10942.2003.
38. Richard DJ, Bolderson E, Khanna KK. 2009. Multiple human single-stranded DNA binding proteins function in genome maintenance: structural, biochemical and functional analysis. Crit Rev Biochem Mol Biol 44:98–116. https://doi.org/10.1080/10409230902849180.
39. Marceau AH. 2012. Functions of single-strand DNA-binding proteins in DNA replication, recombination, and repair. Methods Mol Biol 922:1–21.

40. Wu Y, Lu J, Kang T. 2016. Human single-stranded DNA binding proteins: guardians of genome stability. Acta Biochim Biophys Sin (Shanghai) 48:671–677. https://doi.org/10.1093/abbs/gmw044.
41. Mohni KN, Smith S, Dee AR, Schumacher AJ, Weller SK. 2013. Herpes simplex virus type 1 single strand DNA binding protein and helicase/primase complex disable cellular ATR signaling. PLoS Pathog 9:e1003652. https://doi.org/10.1371/journal.ppat.1003652.
42. Weller SK, Coen DM. 2012. Herpes simplex viruses: mechanisms of DNA replication. Cold Spring Harb Perspect Biol 4:a013011. https://doi.org/10.1101/cshperspect.a013011.
43. Darwish AS, Grady LM, Bai P, Weller SK. 2015. ICP8 filament formation is essential for replication compartment formation during herpes simplex virus infection. J Virol 90:2561–2570. https://doi.org/10.1128/JVI.02854-15.
44. Yao XD, Evans DH. 2003. Characterization of the recombinant joints formed by single-strand annealing reactions in vaccinia virus-infected cells. Virology 308:147–156. https://doi.org/10.1016/S0042-6822(02)00089-2.
45. Hamilton MD, Evans DH. 2005. Enzymatic processing of replication and recombination intermediates by the vaccinia virus DNA polymerase. Nucleic Acids Res 33:2259–2268. https://doi.org/10.1093/nar/gki525.
46. Senkevich TG, Katsafanas G, Weisberg A, Olano LR, Moss B. 12 September 2017. Identification of vaccinia virus replisome and transcriptome proteins by iPOND coupled with mass spectrometry. J Virol https://doi.org/10.1128/JVI.01015-17.
47. DeMasi J, Du S, Lennon D, Traktman P. 2001. Vaccinia virus telomeres: interaction with the viral I1, I6, and K4 proteins. J Virol 75:10090–10105. https://doi.org/10.1128/JVI.75.21.10090-10105.2001.
48. Koonin EV, Senkevich TG, Chernos VI. 1993. Gene A32 product of vaccinia virus may be an ATPase involved in viral DNA packaging as indicated by sequence comparisons with other putative viral ATPases. Virus Genes 7:89–94. https://doi.org/10.1007/BF01702351.
49. Iyer LM, Makarova KS, Koonin EV, Aravind L. 2004. Comparative genomics of the FtsK-HerA superfamily of pumping ATPases: implications for the origins of chromosome segregation, cell division and viral capsid packaging. Nucleic Acids Res 32:5260–5279. https://doi.org/10.1093/nar/gkh828.
50. Unger B, Traktman P. 2004. Vaccinia virus morphogenesis: A13 phosphoprotein is required for assembly of mature virions. J Virol 78:8885–8901. https://doi.org/10.1128/JVI.78.16.8885-8901.2004.